Arabian Journal of Chemistry (2014) 7, 319–326

King Saud University

Arabian Journal of Chemistry

www.ksu.edu.sa
www.sciencedirect.com

ORIGINAL ARTICLE

Experimental, Monte Carlo and molecular dynamics simulations to investigate corrosion inhibition of mild steel in hydrochloric acid solutions

K.F. Khaled [a,b,*], A. El-Maghraby [b,c]

[a] Electrochemistry Research Laboratory, Ain Shams University, Faculty of Education, Chemistry Department, Roxy, Cairo, Egypt
[b] Materials and Corrosion Laboratory, Taif University, Faculty of Science, Chemistry Department, Taif, Hawiya 888, Saudi Arabia
[c] Ceramic Department, National Research Center, Dokki, Giza, Egypt

Received 7 October 2010; accepted 13 November 2010
Available online 18 November 2010

KEYWORDS

Corrosion inhibition;
Furan derivatives;
Mild steel;
Adsorption;
Molecular dynamics simulation

Abstract The efficiency of three furan derivatives, namely 2-(*p*-toluidinylmethyl)-5-methyl furan (Inh. A), 2-(*p*-toluidinylmethyl)-5-nitro furan (Inh. B) and 2-(*p*-toluidinylmethyl)-5-bromo furan (Inh. C), as possible corrosion inhibitors for mild steel in 1.0 M HCl, has been determined by weight loss and electrochemical measurements. These compounds inhibit corrosion even at very low concentrations, and 2-(*p*-toluidinylmethyl)-5-methyl furan (Inh. A) is the best inhibitor. Polarization curves indicate that all compounds are mixed-type inhibitors, affecting both cathodic and anodic corrosion currents. Adsorption of furan derivatives on the mild steel surface follows the Langmuir adsorption isotherm, and the calculated Gibbs free energy values confirm the chemical nature of the adsorption. Monte Carlo simulations technique incorporating molecular mechanics and molecular dynamics can be used to simulate the adsorption of furan derivatives on mild steel surface in 1.0 M HCl.

1. Introduction

The study of corrosion of mild steel and iron is a matter of tremendous theoretical and practical concern and as such has received a considerable amount of interest (Uhlig and Revie, 1985; Sastri, 1998).

Acid solutions, widely used in industrial acid cleaning, acid descaling, acid pickling, and oil well acidizing, require the use of corrosion inhibitors in order to restrain their corrosion attack on metallic materials. The use of organic compounds containing oxygen, sulfur and nitrogen to reduce corrosion attack on steel has been studied in some details (Sykes, 1990; Elachouri et al., 1995; Mernari et al., 1998). The existing data

* Corresponding author. Permanent address: Electrochemistry Research Laboratory, Ain Shams University, Faculty of Education, Chemistry Department, Roxy, Cairo, Egypt.
E-mail address: khaledrice2003@yahoo.com (K.F. Khaled).
Peer review under responsibility of King Saud University.

Production and hosting by Elsevier

1878-5352 © 2010 Production and hosting by Elsevier B.V. on behalf of King Saud University.
http://dx.doi.org/10.1016/j.arabjc.2010.11.005

show that most organic inhibitors adsorb on the metal surface by displacing water molecules on the surface and forming a compact barrier film (Phani et al., 1995).

The interfacial behaviour of organic compounds can be modeled by modifying substituent and functional groups. Molecules that are otherwise only physically attached to the metal surface can be changed into chemically adsorbed entities. This is of particular significance in the field of corrosion inhibitors.

The correlation between the inhibitor efficiency and the molecular structure of organic compounds has been extensively investigated (Kuron et al., 1985; Edwards et al., 1994; Sastri and Perumareddi, 1994; Stupniek-Lisac et al., 1995).

Availability of non-bonded (lone pair) and π-electrons in inhibitor molecules facilitates electron transfer from the inhibitor to the metal. A coordinate covalent bond involving transfer of electrons from inhibitor to the metal surface may be formed (Hackerman and Hurd, 1962). The strength of the chemisorption bond depends upon the electron density on the donor atom of the functional group and also upon the polarizability of the group.

The present work involves an extensive investigation of the three furan derivatives, which have been chosen to evaluate the effect of systematic changes in the molecular structure and the polar function of the compound. This is achieved by changing the substituents with respect to the oxygen hetero-atom in the furan ring, using one type of substituent.

This study aims to continue our pervious investigation of furan derivatives as possible corrosion inhibitors (Khaled, 2010a) for mild steel in 1.0 M HCl solutions. Measurements were conducted using several corrosion monitoring techniques, such as weight loss, potentiodynamic polarization, and electrochemical impedance spectroscopy, EIS. It is also the purpose of this paper to elucidate the adsorption behaviour of some furan derivatives at the mild steel surface using molecular dynamics simulations.

2. Experimental details

The furan derivatives investigated as corrosion inhibitors in hydrochloric acid are presented in Fig. 1. All furan derivatives were prepared by sodium borohydride reduction of corresponding azomethynes according to reported procedure (Klepo and Jakopi, 1985, 1987; Hansal et al., 1955).

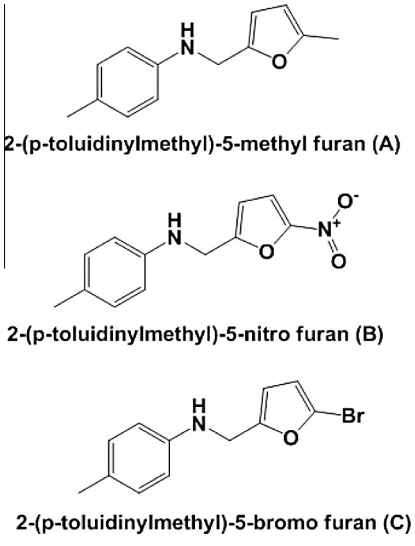

Figure 1 Investigated furan derivatives.

The aggressive solution (1.0 M HCl) was prepared by dilution of analytical grade 37% HCl solution with double-distilled water. Prior to all measurements, the steel samples with the following composition (0.09% P; 0.38% Si; 0.01% Al; 0.05% Mn; 0.21% C; 0.05% S and the remainder iron) were abraded with different emery paper up to 4/0 grit size, washed thoroughly with double-distilled water, degreased with AR grade ethanol, acetone and dried at room temperature.

Weight loss measurements were carried out in a double walled glass cell equipped with a thermostat-cooling condenser. The solution volume was 100 ml. The steel specimens used had a rectangular form (2.5 cm × 2 cm × 0.05 cm). The immersion time for the weight loss was 6 h at 30 ± 1 °C. After the corrosion test, the specimens of steel were carefully washed in double-distilled water, dried and then weighed. The rinse removed loose segments of the film of the corroded samples. Triplicate experiments were performed in each case and the mean value of the weight loss is reported. Weight loss allowed us to calculate the mean corrosion rate as expressed in mg cm^{-2} h^{-1}.

The electrochemical measurements were performed in a typical three-compartment glass cell consisted of the mild steel specimen as working electrode (WE), platinum counter electrode (CE), and a saturated calomel electrode (SCE) as the reference electrode. The counter electrode was separated from the working electrode compartment by fritted glass. The reference electrode was connected to a Luggin capillary to minimize IR drop. Solutions were prepared from bidistilled water of resistivity 13 MΩ cm.

The electrode potential was allowed to stabilize 60 min before starting the measurements. All experiments were conducted at 30 ± 1 °C. Measurements were performed using Gamry Instrument Potentiostat/Galvanostat/ZRA. This includes a Gamry Framework system based on the ESA400, Gamry applications that include dc105 for dc corrosion measurements, EIS300 for electrochemical impedance spectroscopy measurements along with a computer for collecting data. Echem Analyst 5.58 software was used for plotting, graphing and fitting data.

Tafel polarization curves were obtained by changing the electrode potential automatically from (−750 to −300 mV_{SCE}) at open circuit potential with scan rate of 1.0 mV s^{-1}. Impedance measurements were carried out in frequency range from 10 kHz to 20.0 mHz with an amplitude of 10 mV peak-to-peak using ac signals at open circuit potential.

The values of inhibition efficiency from corrosion current density and charge transfer resistance were calculated using Eqs. (1) and (2), respectively.

$$\sigma_p\% = \frac{j^o_{corr} - j_{corr}}{j^o_{corr}} \times 100 \quad (1)$$

where j^o_{corr} and j_{corr} are corrosion current densities obtained in the absence and presence of inhibitor, respectively:

$$\sigma_{EIS}\% = \frac{R_{ct} - R^o_{ct}}{R_{ct}} \times 100 \quad (2)$$

where R_{ct} and R^o_{ct} are charge transfer resistances in the presence and absence of inhibitor, respectively.

3. Computational details

The Discover molecular dynamics module in Materials Studio 4.3 software from Accelrys Inc. (Barriga et al., 2007) allows selecting a thermodynamic ensemble and the associated parameters, defining simulation time, temperature and pressuring and initiating a dynamics calculation. The molecular dynamics simulations procedures have been described elsewhere (Khaled, 2010b,c).

4. Results and discussion

4.1. Chemical methods

4.1.1. Weight loss measurements

Fig. 2 shows the variation of the corrosion rate (in mg cm^{-2} h^{-1}) of a mild steel electrode in 1.0 M HCl solutions without and with various concentrations (0.5–20 mM) of furan derivatives at 30 °C. The weight loss per unit time; mg cm^{-2} h^{-1} represents the corrosion rate of mild steel at the specified conditions. From these data, the weight loss (and hence the rate of corrosion) of the mild steel electrode decreases with increasing furan derivatives concentration, as indicated in Table 1. This is clearly seen from Fig. 2 the decrease in corrosion rate with increase in inhibitor concentration. This trend may result from the fact that adsorption and surface coverage increases with the increase in furan derivatives concentration; thus the surface is separated from the medium (Abdallah et al., 2006; Zhao and Mu, 1999).

The inhibition efficiency (σ_w%) was calculated by the following relation:

$$\sigma_w\% = \frac{W_{corr} - W_{corr(inh)}}{W_{corr}} \times 100 \quad (3)$$

where W_{corr} and $W_{corr(inh)}$ are the corrosion rates of steel in the absence and presence of the furan derivatives, respectively.

Fig. 3 shows the variation of inhibition efficiencies evaluated from weight loss measurements for different inhibitor concentrations in 1.0 M HCl. The corrosion rate decreases with the addition of furan derivatives and in turn the inhibition efficiency (σ_w%) increases to attain values of more than 94%. From weight loss measurements, we can conclude that (Inh. A) is the best corrosion inhibitor compared to Inh. B and Inh. C.

Table 1 Corrosion rate in (mm yr^{-1}) and inhibition efficiency σ_w% data obtained from weight loss measurements for mild steel in 1.0 M HCl solutions in the absence and presence of various concentrations of furan derivatives at 30 ± 1 °C.

Inhibitor	Concentration (mM)	Corrosion rate (mg cm^{-2} h^{-1})	Corrosion rate (mm yr^{-1})	σ_w%
	Blank	1.05	11.8	–
Inh. C	0.5	0.73	8.2	30.2
	10	0.42	4.7	60.3
	15	0.35	3.9	66.4
	20	0.16	1.8	84.2
Inh. B	0.5	0.58	6.5	44.5
	10	0.33	3.7	68.3
	15	0.22	2.4	78.4
	20	0.13	1.4	88.1
Inh. A	0.5	0.45	5.05	56.3
	10	0.23	2.6	78.2
	15	0.14	1.6	86.4
	20	0.06	0.67	94.3

4.2. Electrochemical measurements

4.2.1. Potentiodynamic measurements

The corrosion of mild steel electrode in 1.0 M HCl solutions containing various concentrations of furan derivatives was studied by potentiodynamic polarization. Inhibition efficiency σ_p% was calculated by applying a relationship described in Eq. (1) (Khaled et al., 2000). The anodic and cathodic polarization curves for mild steel in 1.0 M HCl in the absence and presence of inhibitors are shown in Figs. 4–6. As can be seen, both

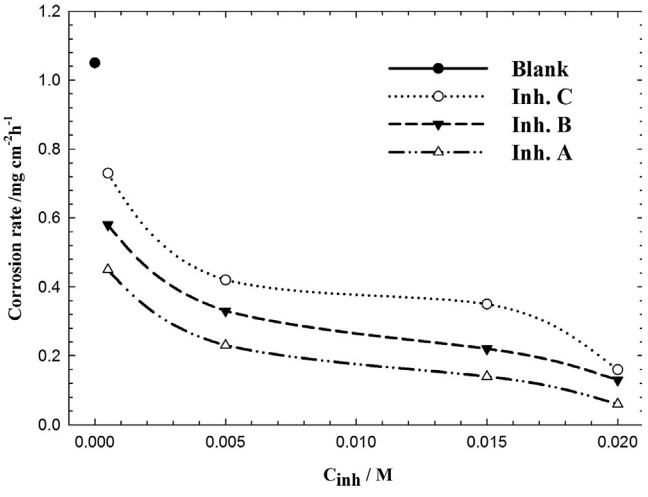

Figure 2 The variation of the weight loss (in mg cm^{-2} h^{-1}) of a mild steel electrode in 1.0 M HCl solutions without and with various concentrations (0.5–20 mM) of furan derivatives at 30 ± 1 °C.

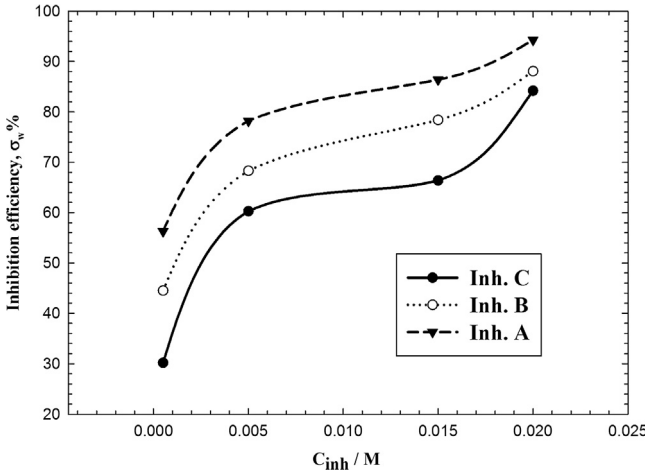

Figure 3 The variation of the inhibition efficiency of a mild steel electrode in 1.0 M HCl solutions without and with various concentrations of furan derivatives at 30 ± 1 °C.

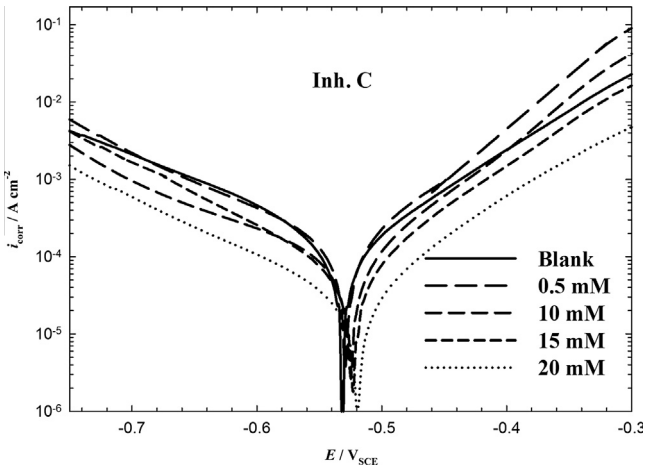

Figure 4 Anodic and cathodic Tafel polarization curves for mild steel in the absence and presence of various concentrations of Inh. C at 30 ± 1 °C.

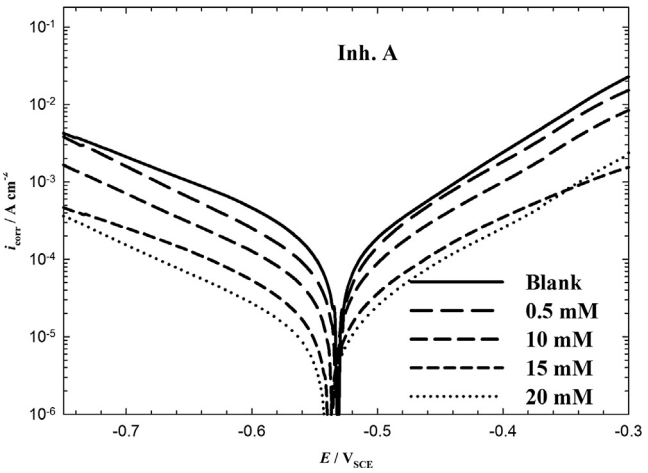

Figure 6 Anodic and cathodic Tafel polarization curves for mild steel in the absence and presence of various concentrations of Inh. A at 30 ± 1 °C.

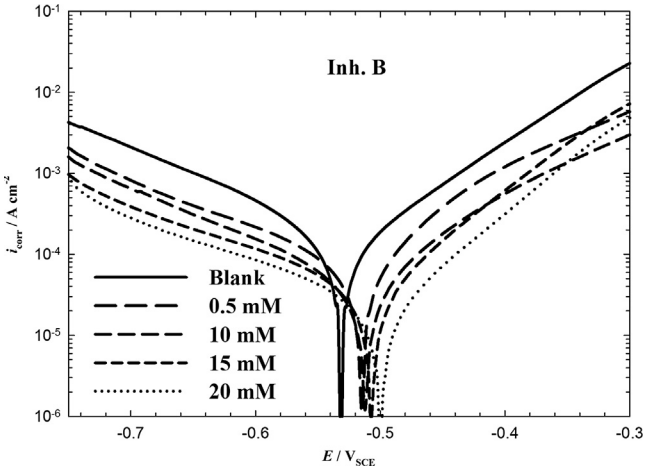

Figure 5 Anodic and cathodic Tafel polarization curves for mild steel in the absence and presence of various concentrations of Inh. B at 30 ± 1 °C.

cathodic and anodic reactions of mild steel electrode were inhibited with the increase of inhibitor concentrations but to different extent. Values of all kinetic parameters such as corrosion potential (E_{corr}), cathodic and anodic Tafel slopes (β_c, β_a) and corrosion current density (j_{corr}) attained by extrapolation of Tafel lines, as well as inhibition efficiency are listed in Table 2.

Clearly, the addition of furan derivatives decreased the corrosion current, j_{corr} significantly for all the concentrations studied. The best inhibition was obtained at 20 mM for all compounds (Figs. 4–6). The variations in inhibition efficiency appears to reflect a structural difference and thus producing the corresponding difference in the nature of interaction between mild steel surface and the respective inhibitor involved. No definite trend was observed in the shift of corrosion potentials. The values of β_c were changed with increasing inhibitor concentration, which indicates the influence of those compounds on the kinetics of hydrogen evolution reaction. The cathodic current *versus* potential gave rise to parallel Tafel lines, representing activated-controlled reaction of the hydrogen

Table 2 Electrochemical kinetic parameters, protection efficiencies (σ_p%) and rates of corrosion associated with Tafel polarization measurements recorded in 1.0 M HCl solutions without and with various concentrations of the three selected Furan derivatives at 30 °C ± 1.

Inhibitor type	[Inhib.] (M)	β_a (mV dec^{-1})	β_c (mV dec^{-1})	$-E_{corr}$ (mV$_{SCE}$)	(j_{corr}) (μA cm^{-2})	σ_p%	Corrosion rate (mm yr^{-1})
	Blank	107	147	531	149	–	1.73
Inh. C	0.5	93.4	130	529	116	22.1	1.3
	10	98.1	156	525	80.9	45.7	0.9
	15	93.7	127	523	69.6	53.3	0.8
	20	108.6	147	520	34.7	76.7	0.4
Inh. B	0.5	117.3	196	515	95.1	36.2	1.1
	10	121.3	178	512	57.5	61.4	0.7
	15	109.8	198	507	42.4	71.5	0.5
	20	112.6	186	500	24.8	83.4	0.3
Inh. A	0.5	102.7	134	532	89.2	40.1	1
	10	104.3	142	535	50.2	66.3	0.6
	15	123.9	172	538	27.8	81.3	0.3
	20	124.1	141	540	11.8	92.1	0.1

evolution. The increase in the anodic Tafel slope β_a is possibly due to changes in the charge transfer coefficient α_a for the anodic dissolution of mild steel, by virtue of the presence of an additional energy barrier due to the presence of the adsorbed inhibitor. Mathematical treatment of such a dual energy barrier was reported first by Mayer (1960) and applied by Conway and Vijh (1967). The rapid attainment of corrosion potential in the presence of the studied furan derivatives suggests that the initial step of adsorption involves the onium cations of the studied furan derivatives (Abdelaal and Morad, 2001). Thus, those compounds can be classified as inhibitors of mixed-type.

4.2.2. Electrochemical impedance measurements

The effect of the concentration of the studied furan derivatives was studied from 5 to 20 mM in 1.0 M HCl solutions at 30 °C ± 1. Organic compounds are known to yield unreliable and irreproducible results for concentrations higher than 20 mM (Donnelly et al., 1978; Trabanelli, 1983). For the same reasons, the present work will test the compounds only up to a concentration of 20 mM.

In the presence of furan derivatives in the whole concentration range, the electrochemical impedance spectra (Nyquist plots) are characterized by one semicircle, whose centre lies under the real axis (Figs. 7–9). The quantitative analysis of the electrochemical impedance spectra was studied based on a physical model of the corrosion process with hydrogen depolarization and with charge transfer controlling step. The simplest model includes the polarization resistance R_{ct} in parallel to the constant phase element (CPE) connected with the solution resistance R_s. The solid electrode is inhomogeneous both on a microscopic and macroscopic scale and corrosion is a uniform process with fluctuating active and inactive domains where anodic and cathodic reactions take place at the corroding surface. The size and distribution of these domains depend on the degree of surface inhomogeneities. Inhomogeneities may arise also from adsorption phenomena, formation of porous and non-porous layers by passivation on coating (Donnelly et al., 1978; Trabanelli, 1983; Stoynov et al., 1991). For this reason the frequency distributed constant phase element was used instead of the capacitance of the double layer C_{dl} at the mild steel/solution interface. More generally, the CPE behaviour could be treated as a "ω space fractality", i.e., as manifestation of a self-similarity in the frequency domain (Stoynov, 1990). The CPE impedance is given by (Stoynov et al., 1991; Stoynov, 1990; Growcock and Jasinski, 1989; Pang et al., 1990; Juttner, 1990; Macdonald, 1987):

$$Z_{CPE} = \frac{1}{(i\omega)^n A} \tag{4}$$

where A is a proportionality coefficient and n has the meaning of the phase shift, whose value can be considered as a measure of the surface inhomogeneity (Stoynov et al., 1991; Growcock and Jasinski, 1989; Lopez et al., 2003; Rammelt and Reinhard, 1987). The transfer function is thus represented by an equivalent circuit, having only one time constant (Fig. 10). Parallel to the double layer capacitance (modeled by a CPE) is the polarization resistance R_p, R_s being the electrolyte resistance. The fitted parameter values are presented in Table 3, while the

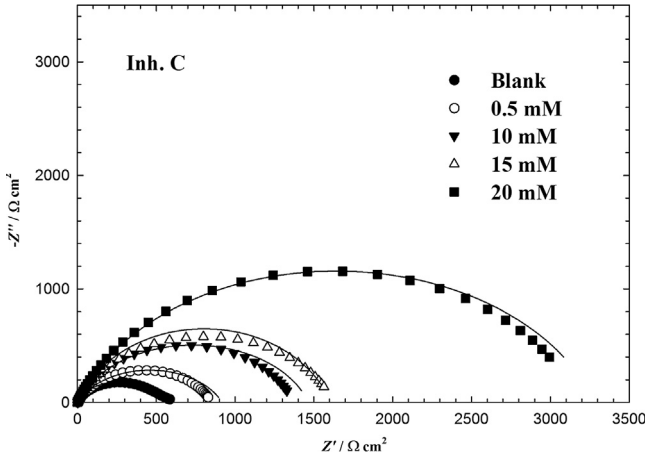

Figure 7 Measured and simulated complex plane impedance plots of mild steel corrosion in 1.0 M HCl solutions at E_{corr} in the absence and presence of Inh. C at 30 ± 1 °C.

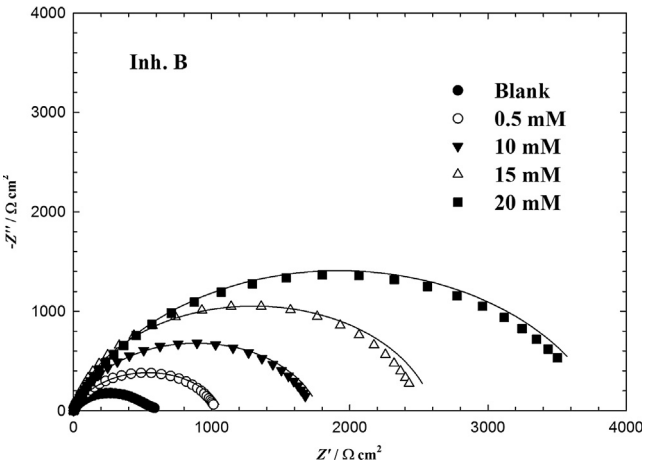

Figure 8 Measured and simulated complex plane impedance plots of mild steel corrosion in 1.0 M HCl solutions at E_{corr} in the absence and presence of Inh. B at 30 ± 1 °C.

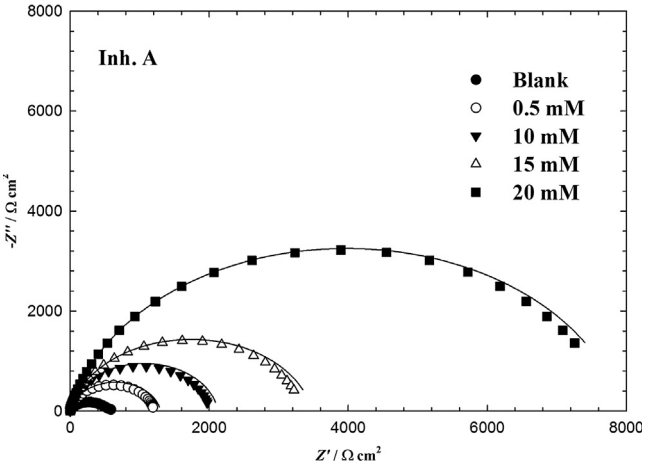

Figure 9 Measured and simulated complex plane impedance plots of mild steel corrosion in 1.0 M HCl solutions at E_{corr} in the absence and presence of Inh. A at 30 ± 1 °C.

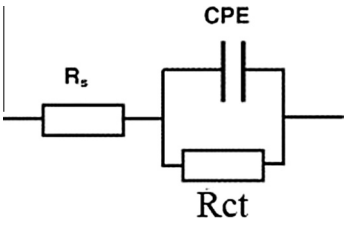

Figure 10 Equivalent circuit model for the corrosion of mild steel electrode.

calculated curves, presented in Figs. 7–9 as solid lines while the experimental values represented as symbols.

4.3. Adsorption isotherm

The adsorption of organic molecules provides information about the interaction among the adsorbed molecules themselves as well as their interaction with the electrode surface. Corresponding chemisorptions mechanism can occur, accompanied by the displacement of water molecules from the metal surface and sharing the lone pair of electrons between the hetero-atoms and/or the aromatic system and the mild steel surface. In addition, the cationic form of the studied furan derivatives are capable of adsorption through electrostatic interactions influenced by the chloride anions in acidic solution.

The most frequently used adsorption isotherms are Langmuir, Temkin and Frumkin with the general formula

$$f(\theta, x)\exp(-2a\theta) = KC \tag{5}$$

Plots of the data for each isotherm showed all of investigated compounds agreed with the Langmuir isotherm (Fig. 11) that is given by (Christov and Popova, 2004):

$$\frac{C}{\theta} = \frac{1}{K} + C \tag{6}$$

where K is the adsorption equilibrium constant and θ is the coverage degree.

To calculate the surface coverage; θ (average of surface coverage calculated from different techniques), it was assumed

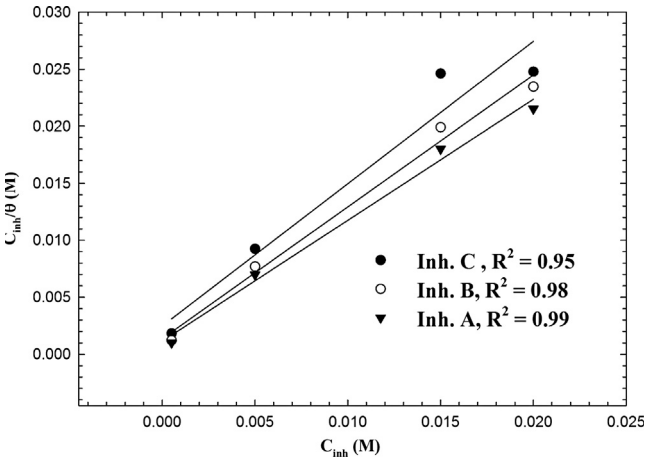

Figure 11 Langmuir adsorption isotherm model for mild steel in 1.0 M HCl containing furan derivatives at 30 ± 1 °C.

that the inhibitor efficiency is due mainly to the blocking effect of the adsorbed species and hence inhibition efficiency = $100 \times \theta$ (Machnikova et al., 2008).

The value of K is related to the standard free energy of adsorption, ΔG°_{ads}, by the following equation (Rafiquee et al., 2008):

$$\Delta G^{\circ}_{ads} = -RT\ln(55.5K_{ads}) \tag{7}$$

where R is the gas constant and T is the absolute temperature. The value of 55.5 is the molar concentration of water in solution expressed in mol l^{-1}.

The values of adsorption constant, slope, and linear correlation coefficient (R^2) can be obtained from the regressions between C/θ and C, and the results are listed in Table 4. The result shows that all the linear correlation coefficients and all the slopes are close to one and confirms that the adsorption of furan derivatives in 1.0 M HCl follows the Langmuir adsorption isotherm. The thermodynamic parameters for adsorption process obtained from Langmuir adsorption isotherms for the studied furan derivatives are given in Table 4. The negative values of ΔG°_{ads} and the higher values of K reveal the spontaneity of adsorption process and they are characteristic of strong

Table 3 Electrochemical parameters calculated from EIS measurements on copper electrode in 1.0 M HCl solutions without and with various concentrations of Furan derivatives 30 ± 1 °C using equivalent circuit presented in Fig. 10.

Inhibitor		R_s (Ω cm^2)	R_{ct} (Ω cm^2)	CPE ($\mu\Omega^{-1}$ cm^{-2} S^n)	n	σ_{EIS}%
	Blank	1.2	599	210	0.73	–
Inh. C	0.5	1.08	849	201	0.75	29.4
	10	1.89	1367	185	0.81	56.2
	15	1.69	1623	177	0.79	63.1
	20	0.59	3186	140	0.80	81.2
Inh. B	0.5	1.36	1034	195	0.81	42.1
	10	0.92	1726	172	0.85	65.3
	15	1.83	2506	160	0.89	76.1
	20	0.93	3767	135	0.80	84.1
Inh. A	0.5	1.21	1202	185	0.93	50.2
	10	1.06	2003	155	0.91	70.1
	15	1.31	3346	138	0.89	82.1
	20	0.79	7790	86	0.88	92.3

Table 4 Thermodynamic parameters for the adsorption of some furan derivatives in 1.0 M HCl on the mild steel at 30 ± 1 °C.

Inhibitor	K (M^{-1})	Slope	R^2	$-\Delta G^{\circ}_{ads}$ (kJ mol^{-1})
Inh. C	401.9	1.1	0.94	25.233
Inh. B	730.9	1.01	0.98	26.73
Inh. A	869.3	1.06	0.99	27.166

interaction and stability of the adsorbed layer with the mild steel surface. The absolute value of the standard free energy of adsorption, ΔG°_{ads}, of the investigated furan derivatives follows the order: Inh. A > Inh. B > Inh. C.

Generally, the energy values of −20 kJ mol^{-1} or less negative are associated with an electrostatic interaction between charged molecules and charged metal surface, physisorption; those of −40 kJ mol^{-1} or more negative involve charge sharing or transfer from the inhibitor molecules to the metal surface to form a coordinate covalent bond, chemisorption (Khamis et al., 1991). The calculated ΔG°_{ads} value, being closer to −20 kJ mol^{-1}, is between the threshold values for physical adsorption and chemical adsorption indicates that adsorption of furan derivatives on steel surface involves the two types of interactions (Behpour et al., 2008).

There are many limitations on the application of Langmuir adsorption isotherm for the analysis of inhibition phenomena and related data. Some of these limitations are discussed below.

Simple adsorption is applicable only under the following conditions:

(a) The surface of the metal is homogeneous.
(b) The adsorbate is specifically adsorbed, and each adsorbed species occupies only a single site of the surface.
(c) There is no surface diffusion of the adsorbed compounds.
(d) The standard free energy of adsorption is independent of the degree of coverage.

The Langmuir adsorption isotherm is somewhat idealized not withstanding the fact that the adsorption may be highly selective with electrode reaction and may be potential-dependent, and the adsorbates may be competitive with water molecules. Adsorption isotherms are none-the-less useful, if the uninhibited corrosion current is in fact proportional to the total number of sites that can possibly adsorb inhibitors. This, however, is not necessarily so, as it is known often that a substantial corrosion rate is observed at a saturation coverage of the inhibitor.

The tested furan derivatives showed a good ability to inhibit the corrosion of mild steel for the tested range of the concentration. They inhibited the corrosion reactions of the substrate active sites by covering them with one or more of the interface adsorbing modes mentioned previously, to form a protective layer of these molecules.

The coverage of inhibitor particles may come out by adsorption (chemisorption), with electron donating or sharing of the polar function of the inhibitors, rather than Van der Waals forces (physisorption), which are known to be reversible and do not yield an effective interface inhibition. The protective chelate-like layer could be monolayer (2-D) of only one or two inhibitor molecules from the metal surface. Formation of 2-D layer on the interface is thought to be the mode of action for this class of compounds due to a combination of primary inhibition (by blocking of active sites. with some indifferent molecules), and secondary inhibition due to the interaction of the adsorbed inhibitor with neighboring adsorbed corrosion products and/or intermediates.

It is believed even if a complexation takes place between these compounds and the corrosion products or intermediates, it will be with a weak formation forces and hardly affecting bonding forces holding the surface atoms in the metal lattice and thus, the possibility of catalyzed reactions is very limited.

4.4. Molecular dynamics simulations

Monte Carlo simulations help in finding the most stable adsorption sites on metal surfaces through finding the low-energy adsorption sites on both periodic and non-periodic substrates or to investigate the preferential adsorption of mixtures of adsorbate components.

Several outputs and descriptors calculated by the Monte Carlo simulation are presented in Table 5. The parameters presented in Table 5 include total energy, in kJ mol^{-1}, of the substrate–adsorbate configuration. The total energy is defined as the sum of the energies of the adsorbate components, the rigid adsorption energy and the deformation energy. In this study, the substrate energy (iron surface) is taken as zero. In addition, adsorption energy in kJ mol^{-1} reports energy released (or required) when the relaxed adsorbate components (furan derivatives) are adsorbed on the substrate. The adsorption energy is defined as the sum of the rigid adsorption energy and the deformation energy for the adsorbate components. The rigid adsorption energy reports the energy, in kJ mol^{-1}, released (or required) when the unrelaxed adsorbate components (i.e., before the geometry optimization step) are adsorbed on the substrate. The deformation energy reports the energy, in kJ mol^{-1}, released when the adsorbed adsorbate components are relaxed on the substrate surface. Table 5 shows also (dE_{ads}/dNi), which reports the energy, in kJ mol^{-1}, of substrate–adsorbate configurations where one of the adsorbate components has been removed.

As can be seen from Table 5, Inhibitor A gives the maximum adsorption energy in negative value found during the simulation process. High values of adsorption energy obtained

Table 5 Outputs and descriptors calculated by the Monte Carlo simulation for adsorption of Furan derivatives on iron (0 0 1).

Inhibitor	Total energy (kJ mol^{-1})	Adsorption energy (kJ mol^{-1})	Rigid adsorption energy (kJ mol^{-1})	Deformation energy (kJ mol^{-1})	dE_{ads}/dNi (kJ mol^{-1})
Inh. C	−195.5	−24.3	−22.0	−2.3	−24.3
Inh. B	−280.3	−26.1	−24.6	−1.5	−26.1
Inh. A	−310.2	−28.2	−27.31	−0.99	−28.2

in case of Inhibitor A molecules explain their highest inhibition efficiency. From the molecular structure of iron, it is evident that the unoccupied d-orbital exhibits a tendency to obtain electron. Furan derivatives, which are discussed in the present work, have a number of lone-pair electrons containing atoms on oxygen atoms, making it possible to provide electrons to the unoccupied orbitals of iron, to form a stable coordination-type bond. Therefore, the studied molecules are likely to adsorb on the iron surface to form stable adsorption layers and protect iron from corrosion.

5. Conclusions

1. The inhibition efficiencies of the three inhibitors obtained from weight loss, potentiodynamic polarization and impedance methods are in good agreement.
2. Potentiodynamic polarization studies have shown that furan derivatives act as mixed-type inhibitors, and their inhibition mechanism is adsorption.
3. Data obtained from EIS measurements were analyzed to model the corrosion inhibition process through appropriate equivalent circuit model, a constant phase element (CPE) has been used.
4. The adsorption of furan derivatives on the steel surface, in 1.0 M HCl solution was found to obey Langmuir's adsorption isotherm with a high negative value of the free energy of adsorption ΔG°_{ads}.
5. Monte Carlo simulations technique incorporating molecular mechanics and molecular dynamics can be used to simulate the adsorption of furan derivatives on iron (0 0 1) surface in 1.0 M HCl.

Acknowledgements

Authors are grateful for the financial support provided by Taif University, Project #1-431-713 and The Center of Research Excellence in Corrosion (CoRE) located at King Fahd University, Project #CR-03-2010, titled: Designing New Corrosion Inhibitors by QSAR and Molecular Dynamics Approaches.

References

Abdallah, M., Helal, E.A., Fouda, A.S., 2006. Corros. Sci. 48, 1639.
Abdelaal, M.S., Morad, M.S., 2001. Br. Corros. J. 36, 253.
Barriga, J., Coto, B., Fernandez, B., 2007. Tribol. Int. 40, 960.
Behpour, M., Ghoreishi, S.M., Soltani, N., Salavati-Niasari, M., Hamadanian, M., Gandomi, A., 2008. Corros. Sci. 50, 2172.
Christov, M., Popova, A., 2004. Corros. Sci. 46, 1613.
Conway, B.E., Vijh, A.K., 1967. J. Phys. Chem. 71, 3637.
Donnelly, B., Downie, T.C., Grzeskowiak, R., Hamburg, H.R., Short, D., 1978. Corros. Sci. 18, 109.
Edwards, A., Osborne, C., Webster, S., Klenerman, D., Joseph, M., Ostovar, P., Doyle, M., 1994. Corros. Sci. 36, 315.
Elachouri, M., Hajji, M.S., Kertit, S., Essasi, E.M., Salem, M., Coudert, R., 1995. Corros. Sci. 37, 381.
Growcock, F.B., Jasinski, R.J., 1989. J. Electrochem. Soc. 136, 2310.
Hackerman, N., Hurd, R.M., 1962. In: Proceedings of the International Congress of Metallic Corrosion. Butterworths, London, p. 166.
Hansal, R., Vargazon, D., Hahn, V., 1955. Arh. Chem. 27, 33.
Juttner, K., 1990. Electrochim. Acta 10, 1501.
Khamis, E., Bellucci, F., Latanision, R.M., El-Ashry, E.S.H., 1991. Corrosion 47, 677.
Khaled, K.F., 2010a. J. Electrochem. Soc. 157, C116–C124.
Khaled, K.F., 2010b. Corros. Sci. 52, 2905.
Khaled, K.F., 2010c. Mater. Chem. Phys. 124, 760.
Khaled, K.F., Abdel-Rehim, S.S., Hackerman, N., 2000. Ann. Univ. Ferrara 2, 713.
Klepo, Z., Jakopi, K., 1985. J. Chem. Eng. Data 30, 237.
Klepo, Z., Jakopi, K., 1987. J. Heterocyclic Chem. 24, 17.
Kuron, D., Botta, A., Gräfen, H., 1985. Werkst. Korros. 36, 407.
Lopez, D.A., Simison, S.N., De Sanchez, S.R., 2003. Electrochim. Acta 48, 845.
Macdonald, J.R., 1987. J. Electroanal. Chem. 223, 25.
Machnikova, E., Whitmire, K.H., Hackerman, N., 2008. Electrochim. Acta 53, 6024.
Mayer, R.E., 1960. J. Electrochem. Soc. 107, 847.
Mernari, B., Elattari, H., Traisnel, M., Bentiss, F., Lagrenee, M., 1998. Corrosion 40, 391.
Pang, J., Briceno, A., Chander, S., 1990. J. Electrochem. Soc. 137, 3447.
Phani, M.K.L.N., Pitchumani, S., Ravichandran, S., Iyer, S.V.K., 1995. J. Electrochem. Soc. 142, 1478.
Rafiquee, M.Z.A., Saxena, N., Khan, S., Quraishi, M.A., 2008. Mater. Chem. Phys. 107, 528.
Rammelt, U., Reinhard, G., 1987. Corros. Sci. 27, 373.
Sastri, V.S., 1998. Corrosion Inhibitors, Principles and Application. John Wiley and Sons, New York.
Sastri, V.S., Perumareddi, J.R., 1994. Corrosion 50, 432.
Stoynov, Z., 1990. Electrochim. Acta 35, 1493.
Stoynov, Z.B., Grafov, B.M., Savova-Stoynova, B., Elkin, V.V., 1991. Electrochemical Impedance. Nauka, Moscow.
Stupniek-Lisac, E., Brnada, A., Mance, A.D., 1995. Corros. Sci. 42, 243.
Sykes, J.M., 1990. Br. Corros. J. 25, 175.
Trabanelli, G., 1983. Personal Communication at the NACE International Corrosion Conference, Dallas, TX.
Uhlig, H.H., Revie, R.W., 1985. Corrosion and Corrosion Control. Wiley, New York.
Zhao, T., Mu, G., 1999. Corros. Sci. 41, 1937.